# Numerical Simulation of Groundwater Flow and Contaminant Transport in the Quaternary Aquifer in 10th of Ramadan City Area, East Delta, Egypt

# المحاكاة العددية لسريان المياه الجوفية وحركة الملوثات بالخزان الرباعي بمنطقة مدينة العاشر من رمضان- شرق الدلتا- مصر

**[1]أحمد الأمين النمر, [2]محمد ابراهيم جاد, [3]ايناس السيد حسين**
[1]كلية الهندسة-جامعة المنصورة
[2] مركز بحوث الصحراء-وزارة الزراعة
[3]مركز بحوث المياة-وزارة الرى

## الملخص :

تعتبر مدينة العاشر من رمضان واحدة من أهم المدن الصناعية الجديدة والتي تقع على بعد 55 كم من القاهرة على طريق مصر-اسماعيلية الصحراوي وقد زاد الاهتمام بهذه المنطقة نظرا لغطائها الصخري المتميز الذي يحتوي على كميات كبيرة من المياه الجوفية ذات الجودة المتوسطة والتربة الصالحة للزراعة. ويهدف البحث إلى دراسة حركة الملوثات بالخزان الجوفي والناتجة من برك الأكسدة والصرف الصناعي بالمنطقة وأثبتت الدراسات وجود تلوث بعناصر الألومنيوم والحديد والاسترانشيوم أعلى من الحد المسموح به. وباستخدام نموذج رياضي مناسب (Visual MODFLOW v 4.2) تم محاكاة حركة الملوثات. وقد أكدت نتائج النموذج إمتداد ريشة تلوث المياه الجوفية مسافات تتراوح من 2 إلى 2.2كم خلال 50 سنة قادمة لتهدد المناطق الزراعية بالمنطقة.

## Abstract :

The establishment of new communities and land reclamation projects in the Egyptian desert areas is one of the most important national targets. One of these areas is the 10th of Ramadan city. The main goal of the study is concerned with delineation of groundwater contaminants plume in the future. The results show that; the ions concentration of most samples from the oxidation ponds resources contain concentrations of $Al^{3+}$, $Cr^{2+}$, $Fe^{2+}$, $Ni^{2+}$ and $Sr^{2+}$ exceeding the acceptable limit of WHO (1996) standards. Also, most of the groundwater samples are polluted with $Al^{3+}$ and $Fe^{2+}$ and $Sr^{2+}$ ions. The infiltration from the oxidation ponds and expansion of reclaimed lands irrigated with wastewater reflect critical environmental hazards. The results of the groundwater flow and transport simulation reveal contamination plume expansion. It will travel 1.8, 2.1 and 2.3 km due NE direction after for $Al^{3+}$, $Fe^{2+}$ and $Sr^{2+}$contaminants respectively. It is strongly recommended that wastes from oxidation ponds must not be used in irrigation without tertiary treatment. The oxidation ponds to minimize the pollution of groundwater with heavy metals is highly recommended.

## Key words:

Hydrogeology, Heavy metals, MODFLOW, Contaminant transport simulation, 10th of Ramadan City.

## 1. INTRODUCTION

In Egypt, great efforts have been done to increase the land reclamation. During the last sixty years, heavy investments have been devoted to turn territories of the unproductive desert into green productive areas, to serve the highly increasing of population. Priorities of land reclamation are given to the west and east Nile delta regions due to the presence of high potential groundwater aquifers of quality and wide plains with deep sandy soil. As a result, the percolation of waste water from domestic industrial or agricultural activities to groundwater depends on the load and behavior of the contaminants as well as geological and hydrogeological factors that control the flow and dispersion of the contaminants. The 10th of Ramadan city is one of the settlements that are constructed on the peripheries near or close to Cairo city to extend the occupational area and to release the socio economic

**Accepted: 7 October 2015**

stresses affecting Cairo due to overpopulation and development practices. The concerned city is located on the fringes of the eastern Nile delta region along Cairo–Ismailia desert road between longitudes 31°30'–32°00' E and latitude 30°00'–30°30'N, with area of about 465 $km^2$. It is bounded by Cairo-Belbies desert road from west, El Shabab canal from east, Ismailia canal from north and Cairo-Ismailia desert road from south. The study area as shown in (Figure1) is characterized by desert climate with arid, hot and rainless summer, and mild winter with scarce amount of precipitation. Since, 1980 the domestic and industrial wastewater of the 10th of Ramadan city has been collected and disposed in three oxidation ponds. Overflow from these ponds is discharged into Wadi El-Watan about 15 km northeast of the city by artificial and natural canals and is collected in lowlands to threat El-Shabab fresh water canal. These accumulated effluents in the lowlands are directly used for irrigation of new reclaimed areas. Oxidation pond No. 1 collects the effluent of domestic wastewater from the urban areas by a rate of 4000$m^3$/day (Table 1). Oxidation pond No. 2 collects domestic and part of the industrial wastewater with an average in flow of about 13000$m^3$/day. Oxidation pond No. 3 collects the effluent from heavy industries at an average flow of about 25000$m^3$/day (Taha et al. 2004). These figures have changed over time.

# 2. Geomorphological and Geological Settings

The geomorphology and geology of the study area has been studied by many authors. Among them Abbas (1953), Shukri (1953), Shukri and Ayouty (1956), Said and Beheri (1961), Soliman and Faris (1963), Shata (1965), El Fayoumy (1968), Shata and El Fayoumy (1970), Ahmed (1977), Kotb (1988), El Fawal and Shendi (1991), Ezz El Deen (1993). These previous studies covered all geomorphologic and geologic settings.

Geomorphologic units in the study area includes El Ankabia-Iweibid structural plain in the south, Bitter lakes and Isthmus plain in the east, Belbies- El Tell El Kabier- El Salhia plains (old deltaic plains) in the north, Wadi El Tumilat depression and Desert dry drainage lines (Figure 2-left). Ground elevation rises from 12 m amsl in the north, to about 180 m amsl in the south. The 10th of Ramadan city is located on the gravelly fluviatile plains. These plains occupy the area west of the cultivated lands of the Nile Delta and extend to Suez Canal.

The geology of the 10th of Ramadan city is composed of sedimentary rocks which belong to Tertiary and Quaternary periods (Figure2-right). Oligocene sands and gravels are well exposed at Gebel El-Hamza and Gebel Um El-Qamar unconformably overly the Upper Eocene sediments. The outcrops of basaltic flows are observed at Gebel Um Raqm and El-Hamza. These basalts are unconformably underlying the marine Miocene sediments. The Pliocene sediments are recorded in the subsurface sections (up to 250 masl). These are composed of rarely fossiliferous dark pyritic clay. The Quaternary sediments cover a major part of the study area. The old wadi deposits of the terraces of the large wadis in the southern portion of the study area are formed of quartz sand, flint and quartzite pebbles.

# 3. Hydrological Settings

The hydrogeologic framework of the study area is described based on the hydrogeological cross-section as shown in (Figure3). The aquifers that have been encountered at the study area during the hydrogeologic investigations of the site include the Quaternary Aquifer of the 10th of Ramadan City Area (QARCA) and the Miocene aquifer (Figure 3). The current understanding of the configuration of the two aquifers and confining clay units shows neither of the two aquifers is continuous for the entire length of the study area, and both are interconnected in

the southern central part of the study area where the groundwater is mixed. Although there is some interconnection between QARCA and Miocene aquifers, they have historically been treated as two separate aquifers (Sallouma, 1983 and Gad et al, 2015). It is likely that groundwater flow in the QARCA and Miocene aquifers at the study area is local, and the flow paths are short (Figure 4).

The combination of the hydraulic barrier to the west, the localized recharge area, and the presence of large Ismailia canal, drains and eastern lakes and Sabkhas surrounding the study area effectively isolates QARCA in the central, northern and eastern parts from the influence of the regional groundwater flow system. The QARCA is unconfined and composed of fluviatile and fluvio-marine graded sand and gravel with clay intercalations of limited extension. It is mainly recharging by seepage from Ismailia canal and the other sub irrigation canals (El-Haddad, 2002; Embaby and El- Haddad 2007). Another local recharge is the infiltration from the oxidation ponds present in the study area The Miocene aquifer is dominated by clastic facies in the southern part of the study area and overlain by about 200 m of Quaternary deposits. This great depth reflects less contamination than QARCA.

The objective of this research was to apply a groundwater model utilizing USGS MODFLOW coupled with solute transport engines to predict the transport and heavy metals contamination from the site.

# 4. Materials and Methods

The numerical simulation of the groundwater flow and solute transport in the QARCA is mainly based on the results of the chemical analyses of 16 water samples collected from the wastewater of the oxidation ponds and groundwater wells in December 2010 and July 2012. Samples were collected using standard EPA methods and transported to the laboratory of the DRC. All collection procedures and analytical methods conform to U.S. EPA protocols (US EPA, 1996). The results beside the archival data from the previous works were collected in order to clarify the main different pollutants from industrial and agricultural activities. Heavy metals were determined using inductively coupled plasma (ICP) apparatus. The used analytical procedures of wastewater samples follow the methods adopted by Rainwater and Thatcher (1960).

The methodology used in this paper depends on the numerical simulation of groundwater flow and solute transport applying Visual MODFLOW software. Visual MODFLOW Premier, a Graphical User Interface (GUI) from Schlumberger Water Services Inc. that uses the USGS MODFLOW computer code was used to build a three-dimensional model of subsurface water flow. The governing equations of the groundwater flow are derived by mathematical combine between the water balance equation and Darcy's law (Anderson and Woessner, 1992). The model describes groundwater flow under non-equilibrium conditions in a heterogeneous and anisotropic medium according to the following equation (Bear, 1979 and Bear & Verruijt 1987):

$$\frac{\partial}{\partial x}\left(K_{xx}\frac{\partial h}{\partial x}\right)+\frac{\partial}{\partial y}\left(K_{yy}\frac{\partial h}{\partial y}\right)+\frac{\partial}{\partial z}\left(K_{zz}\frac{\partial h}{\partial z}\right)-W=S_S\frac{\partial h}{\partial t} \quad (1)$$

Where $K_{xx}$, $K_{yy}$, $K_{zz}$ are values of hydraulic conductivity along the x, y and z coordinate axes ($LT^{-1}$); h is the piezometric head (L); W is a volumetric flux per unit volume and represents source and/or sinks of water ($T^{-1}$); $S_s$ is the specific storage of the porous material ($L^{-1}$) and t is time (T).

The simulation procedure was started by dividing the QARCA domain into a grid pattern of 1500 cells (50 columns and 30 rows). The model cell area covered 1 $km^2$ and included area covers the three oxidation ponds and El-Mahsama Lake and different water bodies. The QARCA was assumed as one complex layer composed of sand and clay intercalations with lateral and vertical facies changes. It was surrounded by fixed head boundary from

north (Ismailia canal), east (Suez fresh water canal), general head boundary from south, and no flow boundary from west. The top and the bottom of the aquifer layer and the boundary conditions were assigned to this grid (Figure5). An annual recharge rate of 14 mm/year and an annual evapotranspiration rate of 2920 mm/year were applied to the model based local data (General Authority of Meteorological Stations, 2000). Oxidation ponds and El-Mahsama Lake were added as lake features, using depths provided by field measurements (3 m). The Ismailia canal was added as a river boundary using an average depth of 4 m (Gad et al, 2015). Both the lake and river boundary areas and shapes were input by tracing the features on the local digital quadrangle.

The surface layer of the model was based on the latest soil survey completed in 2008 (Table 2) by the Desert Research Center (Ismail, 2008). Topographical data were retrieved from the DEM file covered the modeled area with resolution 90mx90m and applied to the surface to show terrain (Figure6). The second layer of the model was designed using values that were calculated from available well logs data. The conductivity was calculated from analysis of available pumping test using a piezometer following standard USGS accepted methods (Fetter, 1994). Porosity and bulk density were collected from (Shata, 1978). The elevation of the QARCA base was determined using the top layer elevation data and using SURFER to subtract 200m from it to represent the assumed thickness of the QARCA. Values that were required for each layer included storativity, specific yield, conductivity, and porosity; they were calculated using equations of pumping test analysis beside available data (Table 3). MODFLOW was set to 18,250 days (50 years approximately) to represent the total time frame required for any sustainable development project.

Model calibration is the process whereby selected model input parameters are adjusted within reasonable limits to produce simulation results that best match the known or measured values. Visual MODFLOW provides a comprehensive selection of model calibration analysis tools for evaluating, interpreting and presenting the model calibration including calculated head versus observed head in both steady and unsteady state. The calibration targets for hydraulic head in the QARCA (Figure 7) were obtained from two synoptic water-level surveys conducted on Dec. 1992, by Gad (1995) and on Dec. 2005, by Gad et al. (2015). This data set was chosen for the quantitative comparisons of simulated versus measured head because it included all of the wells that are within the study area. The model greatly overestimated head in 7 wells and underestimated head in another 3 wells (Fig.7). These wells are located in the south where hydraulic connections in this area are difficult to determine (Gereish 1989, Gereish 1995, Gereish 2003, Gereish 2012, Moheb 2015 and Gereish, 2015). After many times of changing the k value (Table 3) and canceling an observation well, the normalized RMS between the observed and simulated heads was minimized from 42% to 8 % and the calculated head is very closely related to the field observed head (Fig. 7-upper maps). In the process of calibration of transient state, the calibrated groundwater levels of the year 1992 resulting from the steady state simulation are used as starting head to the transient calibration stage in order to reach the field groundwater levels that recorded in 2005 (Gad et al., 2015) so, specific yield values were modified on a trial and errors basis, until a good match between the observed heads of years 1992 & 2005 and the calculated heads were achieved. It can be seen that in general, there is good agreement between the observed and simulated head as normalized RMS value changed from 37.85% to 7.33% (Fig. 7-lower maps).

In addition, simulation of soluble contamination migration by computer is a way to cover the hiatus between field observations and characteristics water movement in porous media. Computer Software can simulate the spatial variability of groundwater flow from one point to other points also show interaction between surface and subsurface water. Along with such process it also possible to monitor and follow the contaminations which exist in groundwater or infiltrated from wastewater oxidation ponds by lateral and/or vertical migration. As contamination moves it disperses. This means that the concentration decreases as it moves far then away from the source of the pollution. For this reason there is different concentration of contaminants at different points in the aquifer. The partial differential equation for three-dimensional of a reactive transport of contaminants in groundwater is given by (Freeze and Cherry 1979):

$$\frac{\partial}{\partial x}\left(D_x \frac{\partial C}{\partial x}\right) - \frac{\partial}{\partial x}(CV_x) - \frac{\partial}{\partial y}(CV_y) + \frac{q}{\theta}C + \sum_{k=1}^{N} R = \frac{\partial C}{\partial t} \quad (2)$$

Where, $C$ is the concentration of contaminant dissolved respective Cartesian co-ordinate axis, $D_{ij}$ is the hydrodynamic dispersion coefficient, $V_i$ is the seepage or linear pore water velocity, $q_s$ is the volumetric flux of water per unit volume of aquifer representing sources (positive) and sinks (negative), $C_s$ is the concentration of the sources or the sinks, θ is the porosity of the porous medium and $R_k$ is chemical reaction term.

Moreover, due to the hydrodynamic dispersion, the concentration of a solute will decrease over distance. Generally speaking, the solute will spread more in the direction of groundwater flow than in the direction normal to the groundwater flow, because longitudinal dispersivity is typically 10 times higher than transverse dispersivity. The transport of a conservative solute in a one-dimensional system can be described by the advection-dispersion equation:

$$\frac{\partial C}{\partial t} = -v\frac{\partial C}{\partial x} + D\frac{\partial 2C}{\partial x2} \quad (3)$$

Where:

$\partial C/\partial t$ is the change in concentration over time, the first term on the right-hand side represents advection and the second term represents hydrodynamic dispersion. The advection-dispersion equation may be solved analytically or numerically under different initial and boundary conditions.

MT3DMS was used to predict heavy metal transport using lead as the surrogate. This engine is the best choice when biodegradation is not a factor when dealing with heavy metals that are persistent (Prommer et al., 2002). The adsorption coefficients were also most appropriate with the MT3DMS engine with heavy metal only having one oxidation state. Geochemical modeling of the Iron concentrations in PHREEQ C-2 indicated that very minimal trivalent iron ($10^{-8}$ mol) would dissociate with the underlying reduced groundwater conditions in this area. Therefore, Iron was used as a surrogate. The initial concentration of Iron was based on the assumption of a constant leakage of 1 mg/l per day for 18,250 days (50 years). This was the estimate of constant leakage from the oxidation ponds since the first complaint in 1988 (Abu Heiba, 1992). A Langmuir sorption curve was used with values calculated from sediment testing and previous studies on similar sediment types. Langmuir was used over Freundlich due to the losses from a single spill incident assumed to be two orders of a magnitude greater through the ground and a very little clay in the soils of the region minimizing additional sorption sites. The model was run using the hydraulic conductivity for the media as calculated as follows:

**K= T/d = 5947/200 = 29.7** m/day horizontally (Table 3). Vertical conductivity was set to 1.72 m per day based on default vertical conductivity solutions from infiltration tests (Table 2) (Gad, 1995, Ismail, 2008 and Gad et al., 2015). Changing of the conductivity,

dispersivity, and adsorption coefficients were done for sensitivity analysis and to parameter adjustment. This process allowed the groundwater model to be delineated for the maximum, minimum, and most probable extent of the plume. The model was run for numerous iterations and outputs were recorded at different time intervals to show the size and extent of the heavy metal plume.

# 5. Results and Discussions

The pH values of the wastewater samples range from 5.8 and 8.9 indicating neutral to slightly high alkaline water while most of the samples are turbid (Table 4). However, some samples are characterized by low turbidity with variable colors, so all these samples have been filtrated before carrying out chemical analysis. Based on the contents of trace elements, heavy metals, minor ions and acceptable contaminant levels, it is clear from Table (4) that the ions concentration of $B^{2+}$, $Ba^{2+}$, $Cd^{2+}$, $Co^{2+}$,$Cu^{2+}$ , $Mn^{2+}$ and $Zn^{2+}$ in all wastewater samples are below the acceptable levels of WHO standard. About 62.5% of the total samples are polluted with $Al^{3+}$ and $Fe^{2+}$ ions. These pollutants may attribute to the wastewater of industrial activities such as Iron and steel factory in $10^{th}$ of Ramadan city as a general. While, all wastewater samples are polluted with $Cr^{2+}$, $Ni^{2+}$ and $Sr^{2+}$. The rest of the elements ($Pb^{2+}$, $V^{2+}$ & $Mo^{2+}$) are below detection limits. This may be due to the precipitation of these elements from aeration in the oxidation ponds.

Moreover, the spatial variation in Al concentrations fluctuated from 0.118 mg/l (July 2012 pond No.2) to 0.458 mg/l (July 2012 pond No.3), in B concentrations fluctuated from 0.269 mg/l (July 2012 pond No.1) to 0.292 mg/l (July 2012 pond No.3), in Cr concentrations fluctuated from 0.034 mg/l (July 2012 pond No.1) to 0.0578 mg/l (July 2012 pond No.3) and from 0.118 mg/l (July 2012 pond No.1) to 4.357 mg/l (July 2012 pond No.3) for Fe concentrations. Total concentrations of Al, Cr, and Fe as high as 0.458, 0.0578 and 4.357 mg/l, respectively, were recorded in oxidation pond No.3, implying contaminated pond (allowable limits are 0.2, 0.05 and 0.3 mg/l respectively).

A comparison of the three oxidation ponds indicated that the wastewater of oxidation pond No.3 seemed to contain higher total Zn and Pb but lower Cu concentrations than those of wastewater of oxidation pond No.1 & No.2. In addition, the temporal variation in pollutant concentration in the wastewater of the present oxidation ponds (Figure8) show significant annual fluctuations for all heavy metals concentration in the three ponds, but no specific trends could be identified. These spatial and temporal variations suggest that the scale and representativeness of sampling require careful planning, and a single sample might not give a satisfactory evaluation of the levels of heavy metal contamination in the three oxidation ponds ecosystems (El-Sayed et al., 2012).

It is important to note that the results of the chemical analysis of the groundwater samples show the presence of the same heavy metals contamination (Table 5). Also, most spatial groundwater contaminants trends within the studied samples appear to be the result of surface water contaminant migration more than rock-water interaction along distinct subsurface flow paths (Figure9). It is concluded, from these discussions, that the concentration of Al, Fe and Sr is higher than that the acceptable limit according to WHO limits. So, the prediction of future concentration of these contaminants is required through applying numerical simulation of the contaminant transportation.

The results of the groundwater flow simulation process (Figure 10) reveal that the implementation impacts of the base case scenario have more or less serious impacts on the QARCA storage and consequently, contamination plume expansion. Figure (10-A) shows the

predicted hydraulic head after time of simulation of 5 years in the cultivated and reclaimed area's drilled wells applying the present development strategy. It is noticed from the figure that, under the exploitation strategy of 1000 $m^3$/day/well (current exploitation scenario), the total drawdown points to 0.2m, in the area adjacent to Ismailia canal as shown in the dashed black curved line characterize wells of groundwater table of 9.6 m (Figure10-A). The decline in the predicted hydraulic head drawdown in the southern part of the QARCA compared with the other aquifer localities may be attributed to the increase in aquifer thickness and increase in sand ratio. Moreover, the decline in the hydraulic head will continue till about 30 years of the simulation period of 50 years. After this interval, the groundwater system in the QARCA will be balanced. Moreover, the QARCA encompasses a large number of "flow domains" related to the appeared drawdown cone after simulation period of 20 years (Figure 10-C), as the pump rate becomes more than the QARCA recharge. This condition will result in piezometeric head decline within the area followed by local groundwater flow from south, east and west directions towards the wells of the El Mullak cultivated area and 6 October for agricultural development company (Figure10-E). There are two cones of depression as a result of high discharge in the west and northeast direction and still increase after 10, 15, 20, 30 years but after 40 years there will be three high discharge zones (Figure10-F).

In addition, to discuss the relation between the changes of the predicted heads in the northeast direction with groundwater travel distance from the oxidation ponds during time of simulation of 50 years (Fig. 11), it is concluded that when the distance increases the head decreases until reaches its minimum value at distance of 28 km from the ponds and then return to increase. Also, when the time increases the head decreases, which reflects an expected increase in the contaminant plume expansion.

Aluminum, Iron and Strontium cannot leach and move with groundwater in the short time because of high absorption capacity of the soil for adsorption of Aluminum, Iron and Strontium particles (Khan and Ansari, 2005) but mobility of them are assumed as the adsorption capacity of the soil is reached. It should be noted that the periods of contaminants migration prediction were selected different (5, 10, 15, 20, 30, 40 and 50 years) to obtain the distinctive results and approving mobility of overloaded Aluminum, Iron and Strontium within the longer time in the study area. This enables the groundwater carried contaminants to bypass the soil particles which permit transportation of high concentrations through the soil (Knapp, 2002 and Saghravani and Mustapha 2011).

From (Figure12) which represents the contaminants predicted movement in QARCA after 50 years of simulation, it is noticed that the contamination is migrating from the oxidation ponds. The source plume appears to be a continuous source plume. The groundwater is moving towards wadi El-Mullak area and 6 October Agriculture Company. The contamination traveled at different distance as mentioned in Table (6). It'll travel 18, 21 and 23 km due NE direction after 50 years of simulation for Al, Fe and Sr contaminant respectively. This means that the contaminant only travels at a speed of about 0.11m/day. The areas will affect by contamination are towards El Shabab canal, wadi El-Mullak area and 6 October Agriculture Company. In addition, there are lateral flow starts after 20 year which threats a great part of the $10^{th}$ of Ramadan city.

# 6. Concologens and Recomendations

The wastewater from both industrial effluents and domestic sewage is drained into three incompletely lined oxidation

ponds and directly used for irrigation of new reclaimed areas. The results show that the oxidation ponds are highly polluted by heavy metals such as Cr2+, Ni2+, Sr2+, Fe2+ and Al2+. The infiltration from the oxidation ponds and expansion of reclaimed lands irrigated with wastewater reflect critical environmental hazards. The results of the groundwater flow and transport simulation reveal contamination plume expansion. It'll travel 18, 21 and 23 km due NE direction after 50 years of simulation for Al, Fe and Sr contaminants respectively. It is highly recommended that wastes from oxidation pond must not be used in irrigation without treatment. New drilled wells should be located far away from pollution sources and observation wells should be installed around oxidation ponds for periodic monitoring.

# References


**[1] Abbas, H.L., (1953):** Contribution to the stratigraphy of the Mokattam Hill and its structure, Cairo, M. Sc. Thesis, Fac. Sci., Alex. Univ., pp. 1-23.

**[2] Abo Haiba, M. F. 1993:** Industrial and agricultural pollution of groundwater in some new communities near Cairo, Egypt. M. Sc., Thesis, Fac. Of Sci., Helwan Univ., 126 P.

**[3] Afify, H.F., (2004):** "Studies on the municipal contamination of water resources in some villages of Ismailia Governorate, Egypt." unpublished Ph. D. Thesis, Suez Canal Univ., Egypt, 151 p.

**[4] Ahmed, S.A., (1977):** The geology of the desert east of Cairo, Bull. Inst. Desert, Egypt, Vol. 111, pp. 42-89.

**[5] Anderson, M. P. and Woessner, W. W. (1992):** "Applied groundwater modeling: Simulation of flow and Advection transport" Academic Press, San Diego, New York Boston, 318 p.

**[6] Bear, J. (1979):** "Hydraulics of Groundwater." McGraw-Hill, New York.

**[7] Bear, J. & Verruijt, A. (1987): "**Modeling Groundwater Flow and Pollution." D. Reidel Publishing Company, Dordrecht, Holland. 414.

**[8] El-Haddad, I. M. (2002)**: Hydrogeological studies and their environmental impact on future management and sustainable development of the new communities and their surroundings, east of the Nile Delta, Egypt. Ph.D. Thesis, Fac. Sci., Mansoura Univ., 435p.

**[9] El Fawal, F.M. and Shendi, E.H., (1991):** Sedimentology and groundwater of the Quaternary sandy layer north of Wadi EI-Tumilat, Ismailia, Egypt, Annals of the Geol. Surv. of Egypt, 17, pp. 305-314.

**[10] El Fayoumy, I.F., (1968):** Geology of groundwater supplies in the region east of the Nile Delta, Ph. D. Thesis, Fac. Sci., Cairo Univ., 201 p.

**[11] Embaby, A.A and El- Haddad, I.M. (2007):** Environmental impact of wastewater on soil and groundwater at the Tenth of Ramadan City area, Egypt. Mansoura Journal of Geology and Geophysics, Vol. 34(2), pp: 25-56.

**[12] El-Sayed, M.H., El-Aassar, A.M., Abo El-Fadl, M.M., and Abd El-Gawad, A.M., (2012):** Hydro-geochemistry and Pollution Problems in 10th of Ramadan City, East El-Delta, Egypt", Journal of Applied Sciences Research, 8(4): 1959-1972.

**[13] Ezz El Deen, H.M., (1993):** Sedimentological and geophysical studies of Heliopolis Basin, Cairo-Ismailia Desert Road and their applications, Egypt, M. Sc. Thesis, Fac. of Sc., Ain Shams Univ., 153

**[14] Fetter, C. W. (1994):** Applied hydrology. Mac Millan.

**[15] Freeze R.A. and Cherry J.A., (1979):** Groundwater, Prentice-Hall, Inc., Englewood Cliffs, New Jersey, U.S.A, p. 604

**[16] Gad, M. I. (1995):** Hydrogeological studies for groundwater reservoirs, east of Tenth of Ramadan City and

vicinities. M. Sc. Thesis, Fac. Sci., Ain Shams Univ., Egypt, 187 p.

**[17] Gad, M. I., El-Kammar, M. M., Ismail, H. M. G., (2015):** Vulnerability Assessment of the Quaternary aquifer of Wadi El-Tumilat, East Delta, Using Different Overlay and Index Methods. AsianReview of Environmental and Earth Sciences. Vol. 2, No. 1, 9-22.

**[18] Geriesh, M. H. (1989):** Hydrogeological investigations of West Ismailia Area, Egypt. M. Sc. Thesis, Fac., of Sci., Suez Canal Univ., Egypt.

**[19] Geriesh, M. H. (1995):** Hydrogeological and hydrogeochemical evalution of groundwater resources at Suez Canal Province, Egypt. Ph. D. Thesis, Suez Canal Univ., Egypt.

**[20] Geriesh, M. H. (2003):** Reconstruction of the paleohydrogeological regime of groundwater flow in the Quaternary aquifers in the Nile Delta, Egypt. 48th Midwest Groundwater Conference, Kalamazoo, W. Michigan University, USA, 1-3 October, 2003.

**[21] Geriesh, B. (2012):** Management of waterlogging problems along Wadi El-Tumilat, Eastern Nile Delta, Using mathematical modeling and GIS techniques, M. Sc. Thesis, Fac., of Sci., Suez Canal Univ., Egypt.

**[22] Geriesh, B. (2015):** CLIMATIC AND HUMAN IMPACTS ON THE HYDROGEOLOGICAL REGIME IN THE EAST OF NILE DELTA, EGYPT. Ph. D. Thesis, Fac., of Sci., Suez Canal Univ., Egypt, 240 P.

**[23] Ismail, H. M. G., (2008):** "Study the vulnerability of groundwater aquifer for pollution in Wadi El-Tumilat, Eastern Delta." Unpublished M.Sc. Thesis, Fac. of Sci., Cairo Univ., 286P.

**[24] Khan and Ansari, 2005:** Eutrophication: an ecological vision. The Botanical Review, 71(4), 449-482, 2005.

**[25] Knapp, 2002:** Nitrogen and Phosphorus: Grolier Educational, ISBN-10: 0717275833; ISBN-13: 978-0717275830**.**

**[26] Kotb, A.M., (1988):** Geological, Hydrogeological and Geo-electrical studies on the eastern portion of Delta, M. Sc. Thesis, Fac. of Sc., Al Azhar Univ., 147 p.

**[27] Moheb, N. M., (2015):** THE IMPACT OF GEOLOGICAL FACTORS ON URBAN PLANNING OF ISMAILIA CITY USING REMOTE SENSING AND GEOGRAPHIC INFORMATION SYSTEM TECHNIQUES. Ph.D. Thesis, Fac. of Sc., Suez Canal Univ., 106 p.

**[28] Nolan, J., Watts, S. and Proctor, B. (2014)**: A Case Study in the Use of 3-Dimensional Ground Water Modeling and Solute Transport Engines as a Tool in Site Assessment. Environment and Pollution; Vol. 3, No. 2; 2014.

**[29] Prommer, H., Barry, D. A., & Davis, G. B. (2002)**: Modeling of physical and reactive processes during biodegradation of a hydrocarbon plume under transient groundwater flow conditions. *Journal of Contaminant Hydrology*, *59*(1-2), 113-131. http://dx.doi.org/10.1016/S0169-7722(02)00078-5

**[30] Rainwater, F.R. and Thatcher, L.L., (1960):** Methods for collection and analysis of water samples, V.S.G.S. water supply, paper No. 1454, 301 p.

**[31] RIGW (1997):** Hydrogeological maps of Egypt scale 1:100,000. Water Research Center, Ministry of Public Works and Water Resources, Egypt.

**[32] Saghravani, S. R. and Mustapha, S., (2011).** Prediction of Contamination Migration in an Unconfined Aquifer with Visual MODFLOW: A Case Study. World Applied Sciences Journal 14 (7): 1102-1106, 2011.

**[33] Said, R. and Beheri, S., (1961):** Quantitative geomorphology of the

area east of Cairo, Bull. Soc. Geographic, Egypt, pp. 121-132.

**[34] Sallouma, M. K. M., (1983):** Hydrogeological and hydrogeochemical studies east of the Nile Delta, Egypt. Ph.D. Thesis, Fac. Sc., Ain Shams Univ., 166p.

**[35] Shata, A.A., (1965**): Geological structure of the Nile Delta. Journ. of Engin. Cairo, (in Arabic), pp. 1-3.

**[36] Shata, A.A.A., (1978):** Genesis, formation and classification of the soils south Ismaelya canal between Belbeis and Ismaelya including Wadi El-Tumilat, M. Sc. Thesis, Fac. Agricul., Zagazig Univ., pp. 1-60.

**[37] Shata, A.A. and El Fayoumy, I.F., (1970):** Remarks on the regional geological structure of the Nile Delta, Symposium Hydrology of Delta, UNESCO, Vol. 1, pp. 189-197.

**[38] Shukri, N.M., (1953**): Geology of the desert area east of Cairo. Bull. Inst. Desert d' Egypte, Vol. 3, No. 2, pp. 89-105.

**[39] Shukri, N.M. and EI-Ayouti, M.K., (1956):** The Geology of Gebel Iwiebid, Gafra area, Cairo Suez District, Bull. Soc. Geographic, Egypt, pp. 67-71.

**[40] Soliman, S.M. and Faris, M.I., (1963):** General geologic setting of the Nile Delta Province, 4th Arab Petrol. Congress, Beirut, pp. 19-28.

**[41] Taha, A. A, El-Mahmoudi, A. S. and El-Haddad, I. M. (2004):** Pollution sources and related environmental impacts in the new communities southeast Nile Delta, Egypt. Emirates Journal for Engineering Research, Vol. 9, No.1, pp: 35-49.

**[42]** US EPA. (1996): Standard Method 1669, Sampling Ambient Water for trace Metals at EPA Water Quality Criteria Levels.

**[43] World Health Organization standards for drinking water (WHO), (1996):** International Standards for drinking water, 3rd edition, Vol. 1, Geneva, Switzerland, 130p.

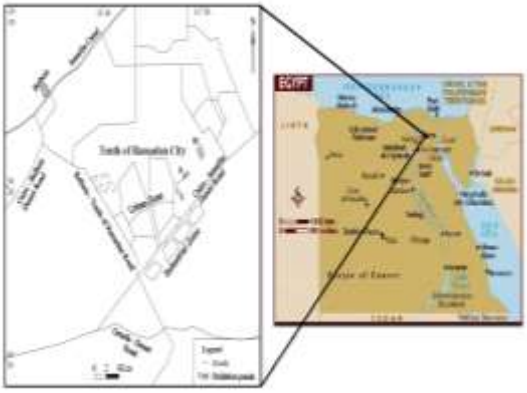

*Figure 1: Location map of the study area*

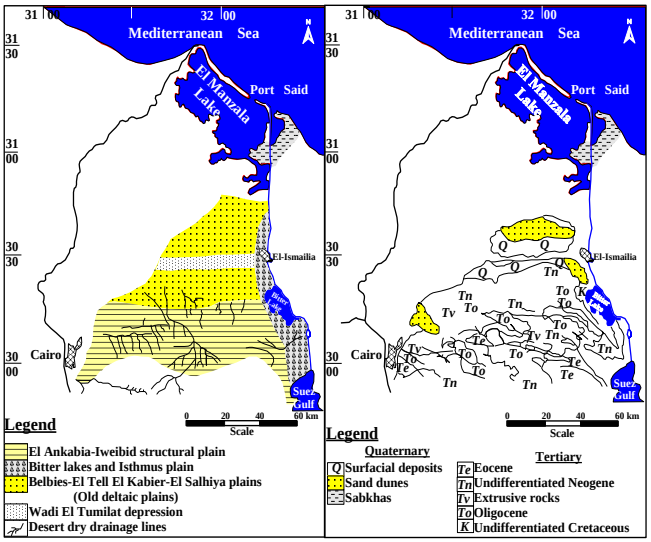


*Figure 2: Geomorphological map (left) and geological map (right) after geological (right map) compiled after geological map of Egypt 1971*

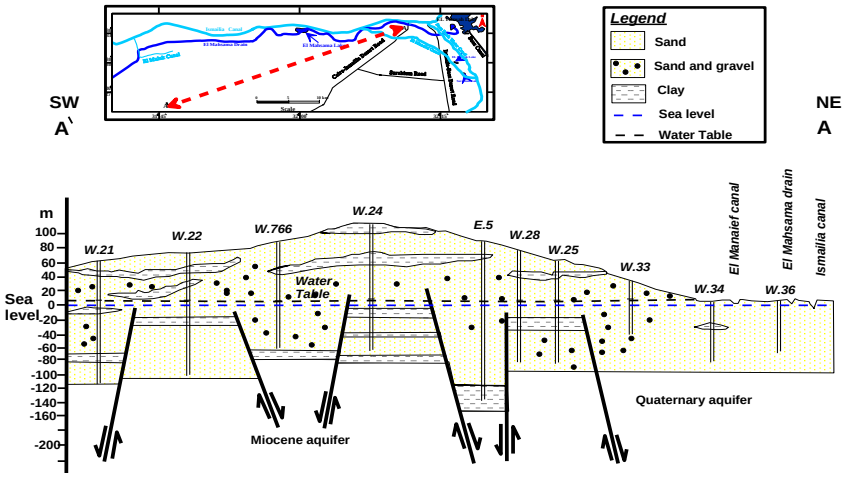


*Figure 3: The cross-section along the QARCA monitoring well line in NE-SW direction showing different water bearing formations (after Gad, 1995)*

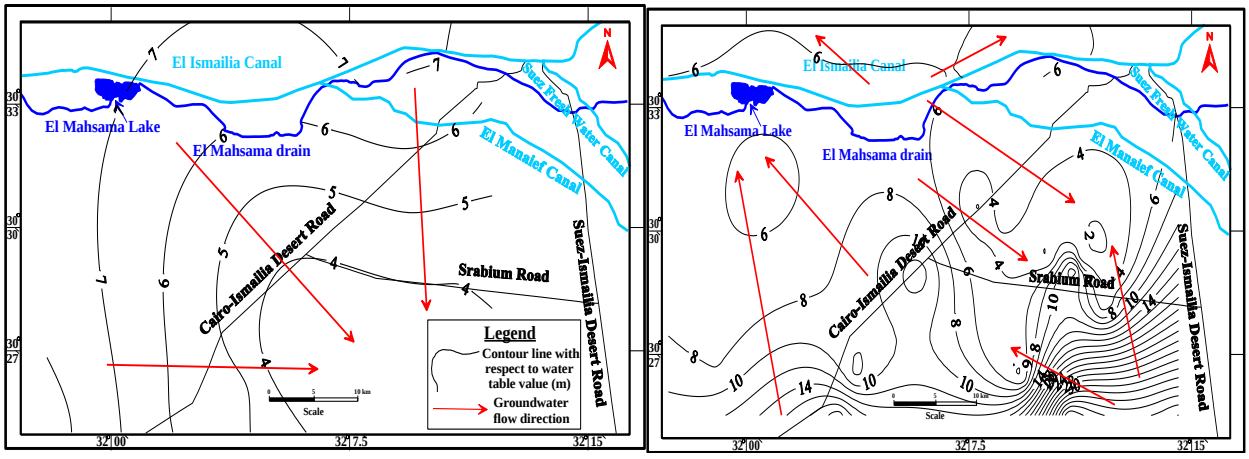


*Figure 4: Water table contour map in Dec. 1992 (left, after Gad 1995) and in Dec. 2005 (right, after Ismail 2008)*

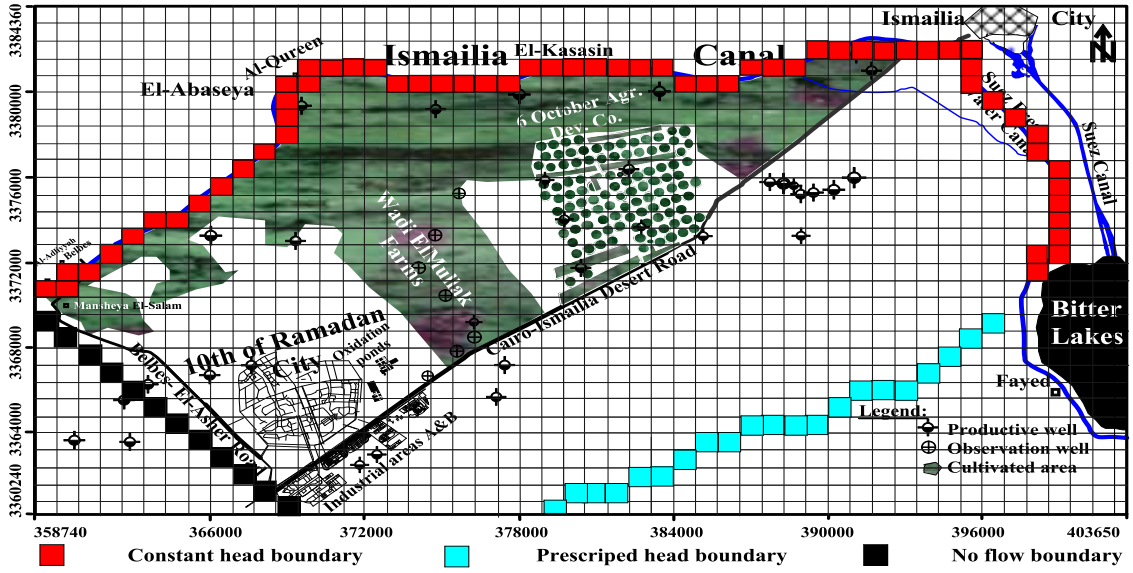


*Figure 5: Finite difference grid and boundary conditions of model domain of QARCA*

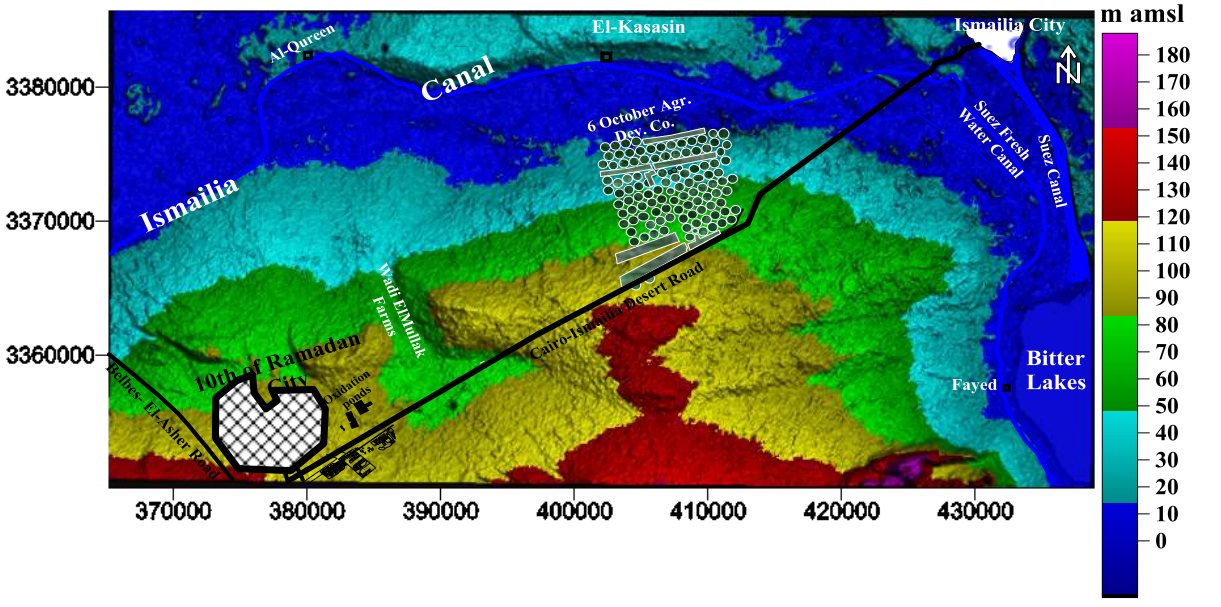


*Figure 6: Ground elevation (m amsl) of QARCA extracted from DEM (Top layer)*

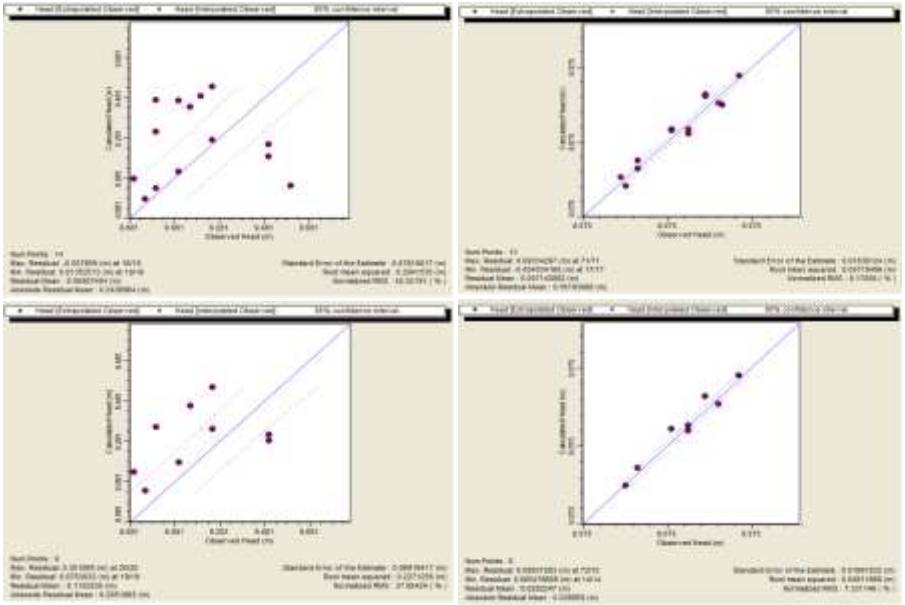

*Figure 7: Steady state calibration results (upper) and transient calibration results (lower)*

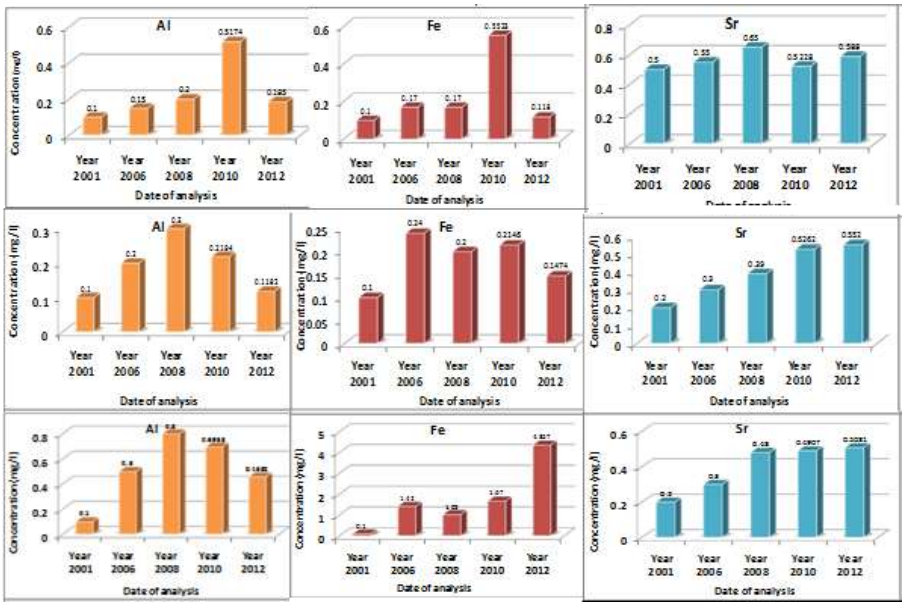


*Figure 8: Temporal variations in Al, Fe and Sr concentrations in Oxidation pond No.1 (upper), Oxidation pond No.2 (middle) and Oxidation pond No.3 (lower)*

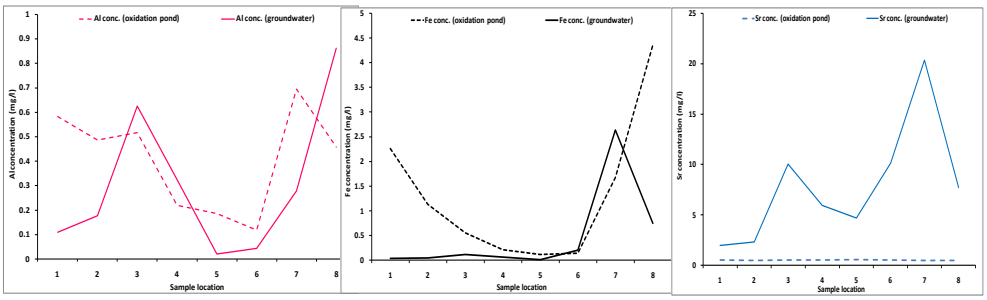


*Figure 9: The general trend of Al contaminant (left), Fe contaminant (middle) and Sr contaminant (right) concentrations in groundwater and surface water samples in the study area*

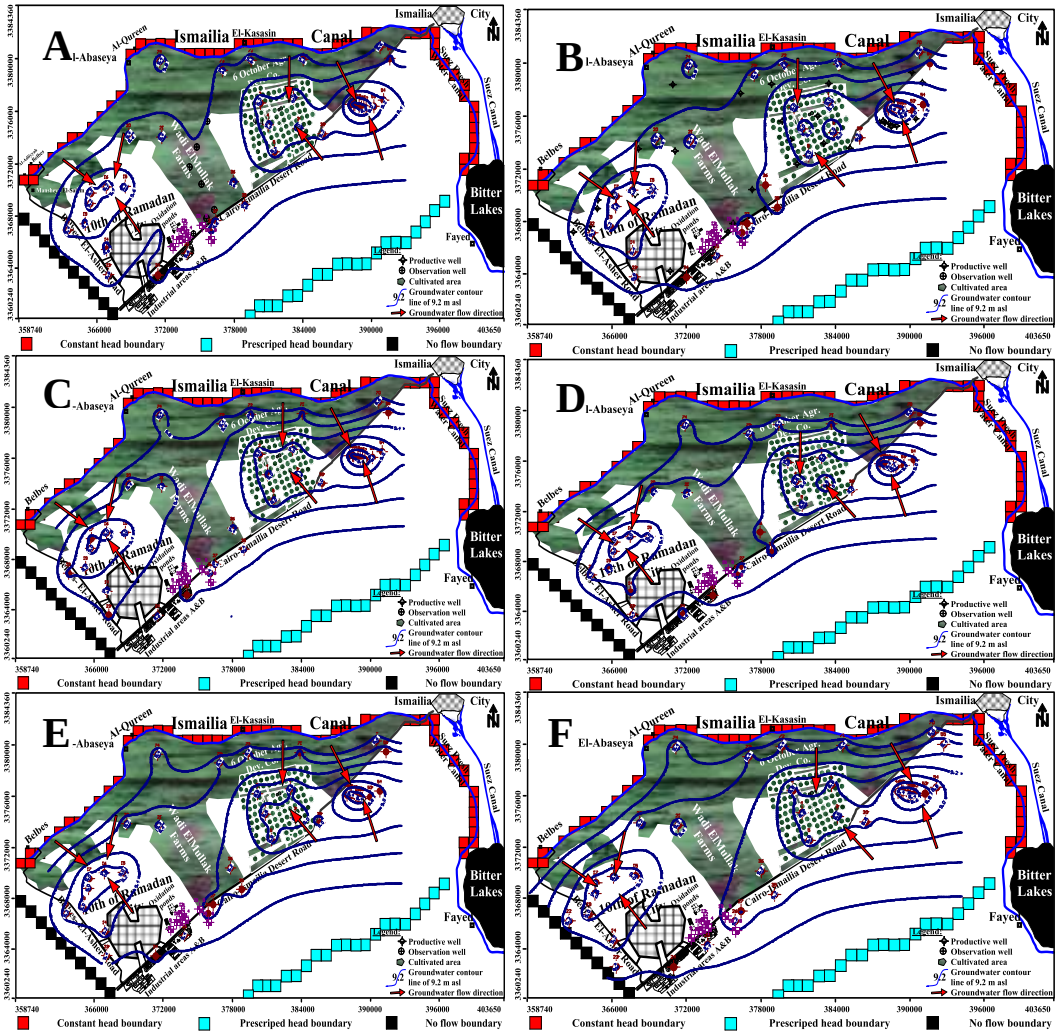


*Figure 10 : Predicted head of CARCA after simulation period of 5 years (A), 10 years (B), 20 years (C), 30 years (D), 40 years (E) and 50 years (F) in CARCA*

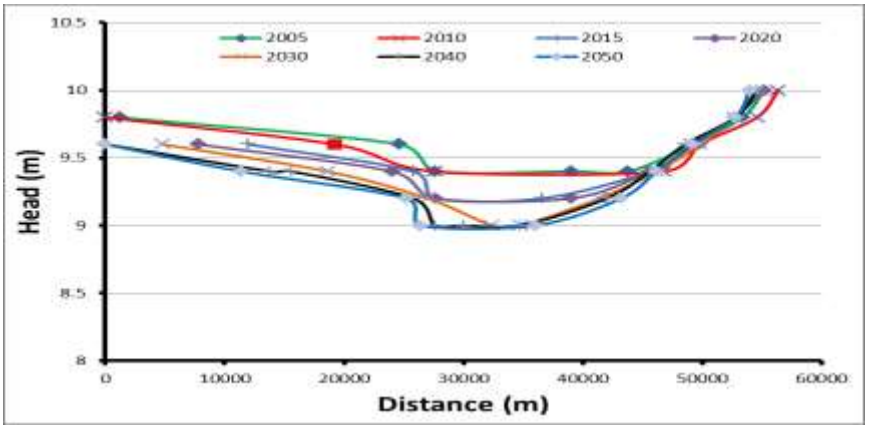


*Figure 11: Predicted head vs distance from the oxidation ponds*

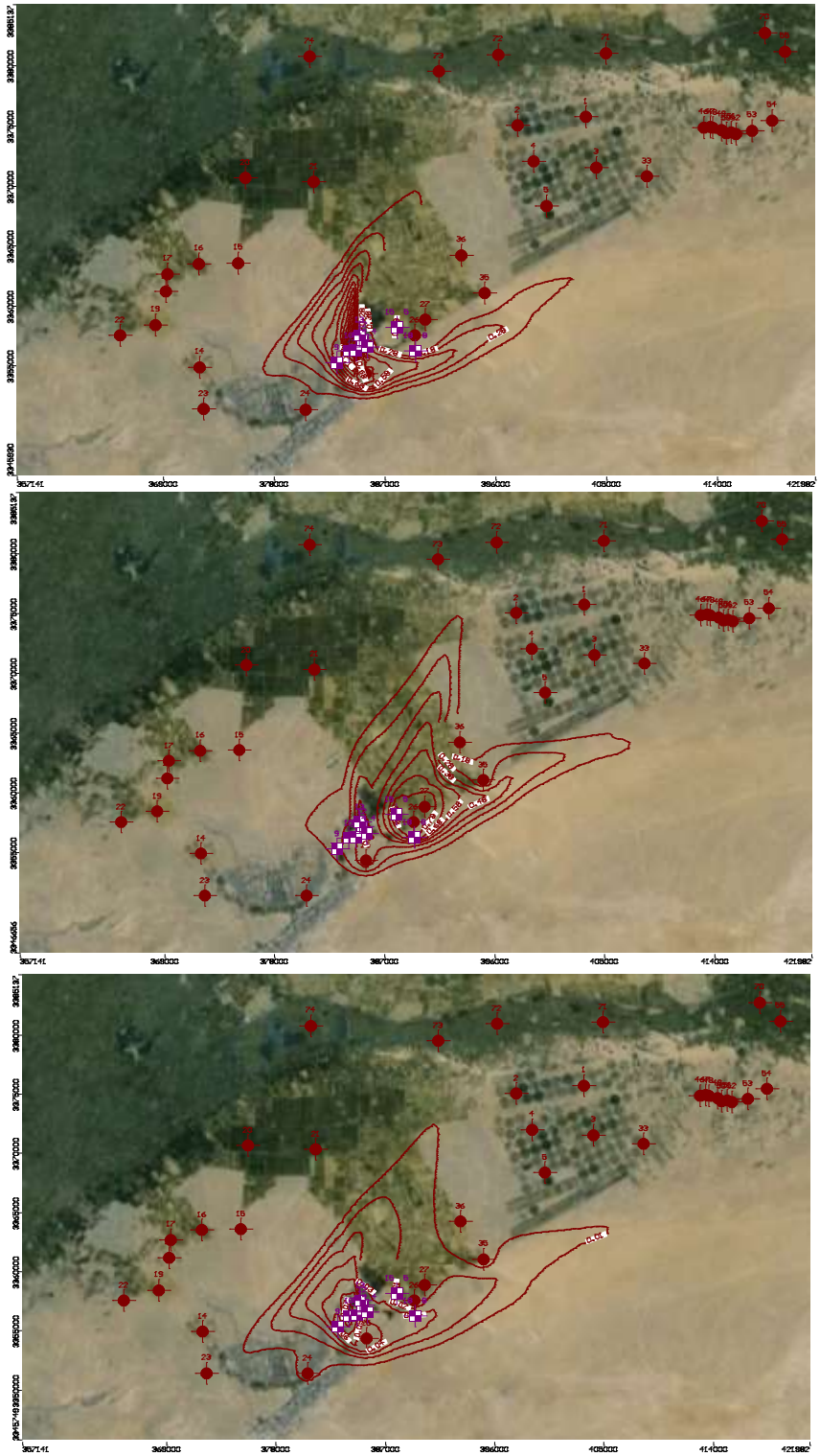

*Figure 12: Predicted plume expansion after 50 years for Aluminum Al (upper), Iron Fe (middle) and Sr (lower)*

*Table 1: Effluent discharges of oxidation ponds in the study area (RIGW, 1997)*

| Pond No. | Number of basins | Area ($m^2$) | Discharge ($m^3$/day) | | Source (%) | |
|---|---|---|---|---|---|---|
| | | | March | April | Domestic | Industrial |
| 1 | 6 | 400,000 | 22,000 | 18,000 | 46 | 54 |
| 2 | 6 | 400,000 | 20,000 | 27,000 | 19 | 81 |
| 3 | 9 | 500,000 | 25,000 | 24,000 | 5 | 95 |

***Table 2: Grain size and infiltration capacities of soil types in QARCA***

| Test no. | Infiltration rate (m/day) | Degree of infiltration | Type of soil based on infiltration rate | Type of soil based on grain size analysis |
|---|---|---|---|---|
| 1 | 1.72*** | Moderately rapid | Good permeability sandy | Gravelly sand soil |
| 2 | 5.872*** | Rapid | sands and loamy sands | Loose sand soil |
| 3 | 0.961*** | Slow | Clays- clay loamy- sandy loamy | Sandy loam soil |
| 4 | 6.335*** | Rapid | sands and loamy sands | Loose sand soil |
| 5 | 1.15* | Moderate | Clays- clay loamy- sandy loamy | Clayey sand soil |
| 6 | 6.03* | Rapid | sands and loamy sands | Loose sand soil |
| 7 | 1* | Moderate | Clays- clay loamy- sandy loamy | Clayey sand soil |
| 8 | 0.08* | Slow | Clays- heavy clays-partially cemented gravels | Sandy loam soil |
| 9 | 4* | Moderately rapid | Good permeability sandy | Gravelly sand soil |
| 10 | 3.36* | Moderately rapid | Good permeability sandy | Gravelly sand soil |
| 11 | 1.31* | Moderate | Clayey sands- clay loams- sandy clay loams | Gravelly sand soil |
| 12 | 1.12* | Moderate | Clayey sands- clay loams- sandy clay loams | Clayey sand soil |
| 13 | 6* | Rapid | sands and loamy sands | Loose sand soil |
| 14 | 1.93 | Moderately rapid | Good permeability sandy loams, sandy clay loams, sandy clays | Gravelly sand soil |
| 15 | 73.296** | Very rapid | Open gravel without soil | Very coarse and gravelly sand |
| 16 | 9.072** | Very rapid | Open gravel without soil | Very coarse and gravelly sand |

*: These data after (Gad, 1995), **: These data after (Afify, 2004), ***: These data after (Ismail 2008)

***Table 3: Hydraulic parameters of QARCA***

| Locality | Transmissivity (T) ($m^2$/day) | Storativity (S) (dimesionless) | Difusivity ($m^2$/day) |
|---|---|---|---|
| QARCA-Northern part | 19986 | 0.0004 | 49965000 |
| QARCA-Northern part | 40600 | 0.0001 | ---- |
| QARCA-Northern part | 20500 | 0.0001 | ---- |
| QARCA-Northern part | 35600 | 0.0011 | ---- |
| QARCA-Middle part | 5947 | 0.0084 | 707976.19 |
| QARCA-Middle part | 17858 | 0.0009 | 19842222 |
| QARCA-Southern part | 9381 | 0.0117 | ---- |
| QARCA-Southern part | 4784 | 0.0025 | 1913600 |
| QARCA-Eastern part | 752 | 0.0003 | 2506666.7 |
| QARCA-Eastern part | 21600 | 0.0145 | 1489655.2 |
| QARCA-Eastern part | 32100 | 0.0208 | 1543269.2 |
| QARCA-Eastern part | 16000 | 0.0097 | |

***Table 4: Results of chemical analysis of wastewater ponds in the study area***

| Pollutant | Recommend Max. Conc. (mg/l) | Location of analysis (December 2010) in mg/l | | | | Location of analysis (July 2012) in mg/l | | | |
|---|---|---|---|---|---|---|---|---|---|
| | | Inflow station | Outflow Station | Pond No.1 | Pond No. 2 | Pond No. 1 | Pond No. 2 | Pond No. 3 | Pond No. 3 |
| **pH** | **----** | **6.8** | **8.9** | **6.4** | **6.4** | **6.7** | **6.8** | **5.8** | **7.6** |
| **E.C.** | **----** | **1358** | **4230** | **1612** | **1563** | **1764** | **2108** | **3520** | **2748** |
| **TDS** | **----** | **922** | **2299** | **1032** | **1000** | **1129** | **1383** | **2253** | **1766** |
| **Al** | **0.2** | **0.583** | **0.487** | **0.517** | **0.219** | **0.185** | **0.118** | **0.695** | **0.458** |
| **B** | **1** | **0.184** | **0.157** | **0.162** | **0.269** | **0.269** | **0.277** | **0.397** | **0.292** |
| **Ba** | **2.0** | **---** | **---** | **0.079** | **0.079** | **0.085** | **0.2545** | **---** | **1.338** |
| **Cd** | **0.005** | **---** | **---** | **0.0007** | **0.0007** | **0.0009** | **0.0006** | **---** | **0.0006** |
| **Co** | **< 0.05** | **---** | **---** | **0.0031** | **0.0031** | **0.003** | **0.0009** | **---** | **0.001** |
| **Cr** | **0.01** | **0.041** | **0.043** | **0.074** | **0.07** | **0.034** | **0.038** | **0.048** | **0.058** |
| **Cu** | **<0.05** | **0.0123** | **<0.009** | **0.0241** | **0.0334** | **0.0109** | **<0.009** | **0.007** | **<0.009** |
| **Fe** | **0.3** | **2.263** | **1.136** | **0.552** | **0.215** | **0.118** | **0.147** | **1.670** | **4.357** |
| **Mn** | **0.2** | **0.105** | **0.065** | **0.092** | **0.095** | **0.067** | **0. 109** | **0.114** | **0.205** |
| **Mo** | **0.05** | **<0.004** | **<0.004** | **<0.0008** | **<0.0008** | **<0.0008** | **<0.004** | **<0.0008** | **<0.004** |
| **Ni** | **0.01** | **0.045** | **0.0389** | **0.056** | **0.045** | **0.034** | **0.032** | **0.032** | **0.047** |
| **Pb** | **0.05** | **<0.006** | **<0.006** | **<0.004** | **<0.004** | **<0.004** | **<0.006** | **<0.004** | **<0.006** |
| **Sr** | **0.11** | **0.535** | **0.491** | **0.528** | **0.526** | **0.588** | **0.552** | **0.491** | **0.508** |
| **V** | **0.01-0.1** | **<0.01** | **<0.01** | **<0.01** | **<0.01** | **<0.01** | **<0.01** | **<0.01** | **<0.01** |
| **Zn** | **5** | **0.245** | **0.178** | **0.117** | **0.047** | **0.026** | **0.021** | **0.122** | **0.141** |

*Table 5: Results of chemical analysis of groundwater of QARCA*

| Parameter | Recommend Maxi. Conc. (Mg/l) (WHO 2004a& 2011) | Henawy Farm (S1) | Tony Farm (S2) | km70 (S3) | km 63 (S4) | Amoon Farm (S5) | Mostafa Farm (S6) | km 60 (S7) | km 55 (S8) | Average |
|---|---|---|---|---|---|---|---|---|---|---|
| Date | | Dec-10 | Dec-10 | Dec-10 | Dec-10 | Jul-12 | Jul-12 | Jul-12 | Jul-12 | |
| pH | | 7.6 | 6.5 | 6.1 | 6.2 | 7.1 | 6.9 | 6.9 | 7.1 | 6.8 |
| E.C. | | 2400 | 4310 | 1035 | 6400 | 8280 | 10930 | 20060 | 7640 | 7631.875 |
| TDS | | 1536 | 2785 | 6624 | 4096 | 5161 | 7035 | 12438 | 4774 | 5556.125 |
| $NO_3$ | 11 | 38 | 54.2 | 100 | 76.4 | 21 | 52.4 | 46.5 | 58.1 | 55.825 |
| $PO_4$ | 1 | 0.0825 | 0.2098 | 0.2935 | 0.1478 | 0.14 | 0.05 | 0.44 | 2.1 | 0.43295 |
| Al | 0.2 | 0.109 | 0.1756 | 0.6249 | 0.3232 | <0.03 | 0.0438 | 0.2776 | 0.8609 | 0.301875 |
| B | 1 | 0.4522 | 1.028 | 2.22 | 0.4837 | 0.6513 | 0.4722 | 0.4201 | 0.506 | 0.779188 |
| Ba | 2 | 0.061 | 0.0721 | 0.0469 | 0.0292 | 0.0785 | 0.1685 | 0.2088 | 0.0775 | 0.092813 |
| Cd | 0.003 | <0.0007 | <0.0007 | <0.0007 | <0.0007 | <0.0006 | <0.0006 | <0.0006 | <0.0006 | BDL |
| Co | <0.05 | <0.001 | <0.001 | <0.001 | <0.001 | <0.0007 | <0.0007 | <0.0007 | <0.0009 | BDL |
| Cr | 0.05 | <0.01 | 0.0263 | <0.01 | <0.01 | 0.0215 | <0.01 | <0.01 | <0.01 | 0.005975 |
| Cu | 1 | <0.003 | <0.003 | 0.0092 | 0.0057 | <0.009 | <0.009 | 0.0332 | 0.0286 | 0.009588 |
| Fe | 0.3 | 0.0405 | 0.0486 | 0.1145 | 0.0625 | <0.02 | 0.207 | 2.633 | 0.7488 | 0.481863 |
| Mn | <0.1 | <0.003 | <0.003 | 0.0098 | 0.0065 | <0.005 | 0.0322 | 0.0578 | 0.0864 | 0.024088 |
| Mo | 0.05 | 0.0019 | <0.0008 | <0.0008 | <0.0008 | <0.004 | <0.004 | <0.004 | <0.004 | BDL |
| Ni | 0.01 | <0.001 | 0.0021 | 0.0038 | 0.0033 | <0.001 | <0.001 | <0.001 | <0.001 | 0.00115 |
| Pb | 0.01 | 0.0064 | 0.0071 | <0.004 | 0.0051 | <0.006 | <0.006 | <0.006 | 0.0144 | 0.004125 |
| Sr | 0.11 | 1.985 | 2.309 | 10.06 | 5.94 | 4.696 | 10.14 | 20.36 | 7.721 | 7.901375 |
| V | 0.01 | <0.01 | <0.01 | <0.01 | <0.01 | <0.01 | <0.01 | <0.01 | <0.01 | BDL |
| Zn | 3 | <0.001 | <0.001 | 0.1338 | 0.0564 | <0.0008 | <0.0008 | 0.2085 | 0.1314 | 0.066263 |

*Table 6: The expected contaminants plume migration distance from the source point (oxidation ponds) after time steps of simulation of 5, 10, 15, 20, 30, 40 and 50 years*

| Pollutant Name | Plume migration in NE direction | | Plume migration in SE direction | |
|---|---|---|---|---|
| | Time (year) | Distance (km) | Time (year) | Distance (km) |
| Al | After 5 years | 15.3 | After 5 years | 13.5 |
| | After 10 years | 16.8 | After 10 years | 15 |
| | After 15 years | 17.4 | After 15 years | 16.5 |
| | After 20 years | 18 | After 20 years | 19.6 |
| | After 30 years | 18.6 | After 30 years | 22.8 |
| | After 40 years | 18.3 | After 40 years | 19.8 |
| | After 50 years | 18.1 | After 50 years | 22.5 |
| Fe | After 5 years | 16.5 | After 5 years | 15 |
| | After 10 years | 18 | After 10 years | 16.5 |
| | After 15 years | 19.5 | After 15 years | 18.3 |
| | After 20 years | 19.8 | After 20 years | 19.8 |
| | After 30 years | 20.4 | After 30 years | 22.2 |
| | After 40 years | 20.7 | After 40 years | 23.4 |
| | After 50 years | 21 | After 50 years | 24 |
| Sr | After 5 years | 18.3 | After 5 years | 16.5 |
| | After 10 years | 20.1 | After 10 years | 18.3 |
| | After 15 years | 21.3 | After 15 years | 19.2 |
| | After 20 years | 21.6 | After 20 years | 21.3 |
| | After 30 years | 22.5 | After 30 years | 24 |
| | After 40 years | 22.8 | After 40 years | 25.8 |
| | After 50 years | 23.4 | After 50 years | 27.6 |